


Spring 5-2016

## Automated Data Acquisition of DEET Time-dependent Concentration Profiles

Ryan D. Coleman  
*University of Southern Mississippi*

Follow this and additional works at: [https://aquila.usm.edu/honors\\_theses](https://aquila.usm.edu/honors_theses)

 Part of the [Chemistry Commons](#), and the [Electrical and Electronics Commons](#)

---

### Recommended Citation

Coleman, Ryan D., "Automated Data Acquisition of DEET Time-dependent Concentration Profiles" (2016).  
*Honors Theses*. 417.  
[https://aquila.usm.edu/honors\\_theses/417](https://aquila.usm.edu/honors_theses/417)

This Honors College Thesis is brought to you for free and open access by the Honors College at The Aquila Digital Community. It has been accepted for inclusion in Honors Theses by an authorized administrator of The Aquila Digital Community. For more information, please contact [Joshua.Cromwell@usm.edu](mailto:Joshua.Cromwell@usm.edu).

The University of Southern Mississippi

Automated Data Acquisition of DEET Time-dependent Concentration Profiles

by

Ryan Coleman

A Thesis  
Submitted to the Honors College of  
The University of Southern Mississippi  
in Partial Fulfillment  
of the Requirements for the Degree of  
Bachelor of Science  
in the School of Computing

May 2016



Approved by

---

Paige Buchanan, Ph.D., Thesis Advisor  
Associate Professor of Chemistry

---

Sabine Heinhorst, Ph.D., Chair  
Department of Chemistry and  
Biochemistry

---

Ellen Weinauer, Ph.D., Dean  
Honors College

## Abstract

Spatial insect repellents must maintain a sufficient concentration in the vapor phase to successfully deter pests. However, little is known regarding correlation of concentration to efficacy nor does there exist a standard testing protocol to measure efficacy in air. Among existing spatial repellents, DEET is the most common active ingredient. This research focuses on application of sensor-based technologies to monitor the concentration levels of DEET under static conditions.

Metal oxide semiconductor sensors feature conductivity variance in response to absorption and desorption of volatile organic compounds. Advantages of these sensors include cost, versatility, and sensitivity. Metal oxide semiconductor sensors were chosen to satisfy the need of forming an array of sensors located at varying distances from an insect repellent sample. However, limitations arise when using metal oxide semiconductor sensors for quantitative purposes due to factors such as nonlinearities of sensor response, memory effects, and sensitivity to environmental factors such as temperature and relative humidity. These limitations were taken into consideration when developing a standard operating procedure for sensor evaluations.

An instrumentation system was developed to monitor the concentration levels of DEET at various distances from the sample over a specified time period. Post processing was performed to analyze sensor response. A first order exponential decay function was used to approximate and compare the time constant of sensor responses.

Key words: electronic instrumentation, gas sensor, metal oxide semiconductor, concentration gradient, spatial repellents, DEET, detection., MOS

## **Dedication**

Dr. Paige Buchanan:

Thank you for involving me in your research efforts  
as well as providing continuous support throughout as my advisor.

It will not be forgotten.

## Acknowledgements

I'd like to thank Dr. Paige Buchanan and Dr. Randy Buchanan for engaging me in this project. Thanks as well to Emily Mathews, Amber Windham, and Brandon Carver for their unwavering support inside the lab.

Special thanks to all three of my great mentors: Dr. Zhaoxian Zhou, Mr. Todd Adams, and Mr. Dan Garcia. You've helped me over several stumbling blocks over the past couple of years, and I'm forever grateful. Lastly, thanks to Anton Netchaev and Biju Bajracharya for serving as role models in their own unique way.

## Table of Contents

List of Figures .....	viii
List of Tables .....	x
List of Equations .....	xi
Chapter 1 – Introduction .....	1
Section 1.1 Spatial Repellants.....	1
Section 1.2 Gas Sensing Technologies .....	1
Section 1.3 Instrumentation System .....	2
Section 1.4 Research Focus .....	3
Chapter 2 – Literature Review .....	3
Section 2.1 Overview of Gas Detection Methods.....	3
Section 2.2 What Makes a Sensor Viable .....	6
Section 2.3 Detection with Metal Oxide Semiconductor Sensors .....	6
Chapter 3 – Methodology .....	9
Section 3.1 Instrumentation Flow .....	9
Section 3.2 Test Chamber Apparatus.....	10
Section 3.3 Sensor Testing Methods.....	10
Section 3.4 Sensor Circuitry .....	12
Section 3.5 Data Acquisition and Processing .....	14
Chapter 4 – Data Analysis .....	17
Section 4.1 – Sensor Resistance Response .....	17
Section 4.2 Normalization .....	20
Section 4.3 Exponential Approximation.....	27
Chapter 5 – Discussion of Results and Conclusions.....	31
Works Cited .....	34



## List of Figures

Figure 1 – Classification of gas sensing methods.....	4
Figure 2 – MOS sensor principle of operation. Absorption of VOC on surface of heated membrane results in a conductivity change of the sensing material.....	5
Figure 3 – MOS response vs FID response. Memory effects of a MOS sensor are evident when compared to an FID response to the same fluctuating gas concentration .....	8
Figure 4 –General system layout containing all principle parts used in implementation of instrumentation system. ....	9
Figure 5 – Temperature controlled 200 mL jacketed flask used as test chamber.....	10
Figure 6 – Basic MOS sensor circuit to monitor the ratio between load resistance and sensor resistance.....	12
Figure 7 – Curve for output voltage as a function of sensor resistance as defined by the voltage divider equation in Equation 2. ....	13
Figure 8 - LabVIEW block diagram for software used in data processing and exportation to CSV.....	14
Figure 9 – Typical sensor voltage response recorded under standard screening protocol for a period of 15 minutes.....	15
Figure 10 – Typical sensor resistance response recorded under standard screening protocol for a period of 15 minutes.....	15
Figure 11 – UltraKera 731 sensor resistance responses to 50 $\mu$ L of DEET at 25 $^{\circ}$ C; 5 cm above sample.....	17
Figure 12 – UltraKera 731 sensor resistance responses to 50 $\mu$ L of DEET at 25 $^{\circ}$ C; 3 cm above sample.....	18

Figure 13 – UltraKera 731 sensor resistance responses to 50 $\mu$ L of DEET at 25 $^{\circ}$ C; 1 cm above sample.....	18
Figure 14 – TGS 2602 sensor resistance responses to 50 $\mu$ L of DEET at 25 $^{\circ}$ C; 5 cm above sample.....	19
Figure 15 – TGS 2602 sensor resistance responses to 50 $\mu$ L of DEET at 25 $^{\circ}$ C; 3 cm above sample.....	19
Figure 16 – TGS 2602 sensor resistance responses to 50 $\mu$ L of DEET at 25 $^{\circ}$ C; 1 cm above sample.....	20
Figure 17 – UltraKera 731 normalized responses to 50 $\mu$ L of DEET at 25 $^{\circ}$ C; 5 cm above sample .....	21
Figure 18 - UltraKera 731 normalized responses to 50 $\mu$ L of DEET at 25 $^{\circ}$ C; 3 cm above sample. ....	21
Figure 19 - UltraKera 731 normalized responses to 50 $\mu$ L of DEET at 25 $^{\circ}$ C; 1 cm above sample. ....	22
Figure 20 – TGS 2602 normalized responses to 50 $\mu$ L of DEET at 25 $^{\circ}$ C; 5 cm above sample. ....	24
Figure 21 – TGS 2602 normalized responses to 50 $\mu$ L of DEET at 25 $^{\circ}$ C; 3 cm above sample .....	24
Figure 22 – TGS 2602 normalized responses to 50 $\mu$ L of DEET at 25 $^{\circ}$ C; 1 cm above sample .....	25

## List of Tables

Data Table 1 – UltraKera 731 Average Response at $t = 90s$ .....	22
Data Table 2 – UltraKera Percent Deviation at $t = 90s$ .....	23
Data Table 3 – TGS 2602 Average Response at $t = 90s$ .....	25
Data Table 4 – TGS 2602 Percent Deviation at $t = 90s$ .....	26
Data Table 5 – UltraKera 731 Time Constants.....	27
Data Table 6 – UltraKera 731 Time Constant Average.....	27
Data Table 7 – UltraKera 731 Time Constant Percent Deviation .....	28
Data Table 8 – TGS 2602 Time Constants .....	29
Data Table 9 – TGS 2602 Time Constant Average .....	29
Data Table 10 – TGS 2602 Time Constant Percent Deviation.....	30

## List of Equations

Equation 1 – Voltage Divider 1 .....	13
Equation 2 – Voltage Divider 2 .....	13
Equation 3 – Sensor Resistance Normalization .....	15
Equation 4 – First Order Exponential Decay .....	16

## **Chapter 1 – Introduction**

### **Section 1.1 Spatial Repellants**

Spatial repellents describe volatile substances applied to various substrates to deter nuisance and biting insects. A requirement of a spatial repellent is that it maintains a sufficient concentration in the vapor phase (Achee 2012). However, little is known regarding the correlation of vapor phase concentration with efficacy, and even less is certain once real world environmental conditions are introduced, such as convection, temperature, relative humidity (RH), and atmospheric pressure.

DEET (diethyltoluamide) is the most common active ingredient in spatial insect repellants (Katz 2007). DEET is a volatile organic compound (VOC), which means it has sufficient vapor pressure to participate in atmospheric reactions. Because the mode of action is spatial repellency, a desirable trait of repellants containing DEET is such that the chemical evaporates over a period of time rather than instantaneously. However, there currently exists no standard measuring technique to assess spatial repellent efficacy. The application of sensor-related technologies to monitor the vapor phase concentration of DEET under static conditions is the focus of this project.

### **Section 1.2 Gas Sensing Technologies**

Advancement in the field of chemical sensors has drastically accelerated over the past three decades. Sensors that detect gases have numerous uses, ranging anywhere from analytical chemistry in a research environment to catalytic combustion detection in an industrial environment (Liu 2012). These sensors or sensor arrays are often adapted to meet the demands of a specific application, which can present technical challenges. Volatile organic compounds can be detected by gas sensing methods, such as sensors

based on the absorption of ionized molecules to a semi-conductive surface, which thereby changes the output of the sensor. Types of gas sensing technology can be typically broken down into four operating principles: electrical, optical, mass sensitive thermometric and calorimetric (Szcurek 2014).

### **Section 1.3 Instrumentation System**

Sensors are a part of the overall instrumentation system, which includes other necessary subsystems. For this particular application, the system is composed of three subsystems: testing chamber, sensing array, and data acquisition.

In order to obtain the readings of the sensors and convert the data into useable values, it was necessary to use a data acquisition (DAQ) device to interface with the sensors. This DAQ device was used to transfer the raw sensor readings to a computer for processing and storage. The data acquisition and processing was performed using custom software developed in Laboratory Virtual Instrument Engineering Workbench (LabVIEW), a graphical programming language prevalent in instrumentation applications. LabVIEW allows the creation of a graphical user interface (GUI), which can be operated by an end user with little knowledge of the underlying code. LabVIEW will allow automated data acquisition and storage.

Both the vapor phase concentration profiles and sensor responses are dependent upon elapsed time and environmental factors. Therefore, it was necessary to adequately control these environmental factors to ensure proper data collection. Solutions for control of temperature and static air conditions (with the exception of the target gas) were investigated to construct an instrumentation system capable of collecting data in a consistent manner with repeatable and accurate results.

## **Section 1.4 Research Focus**

The focus of this research was to design and develop a data sampling system capable of performing automated data acquisition to monitor time dependent concentration profiles of a specific VOC, DEET. Investigations into viable sensors for this application were performed. Multiple sensors of a specific type were tested; sensor efficacy was evaluated using metrics such as sensitivity and response time. Successful sensors were used to monitor the vapor concentration gradient of DEET over a known period of time under ambient conditions.

## **Chapter 2 – Literature Review**

### **Section 2.1 Overview of Gas Detection Methods**

A chemical sensor is a transducer that provides useful information such as the chemical composition or concentration present of a sample. While the term chemical sensor can also include sensors that work with solids and liquids, the focus of this research is on chemical sensors that work with gases.

To form a better understanding of gas sensing technologies, it is helpful to divide sensors into different categories. Liu et al. (2012) divides gas-sensing technologies into two main categories: methods based on electrical variation and non-electrical methods. The sensing material allows further division into more specific techniques. **Figure 1** shows the division of these methods.

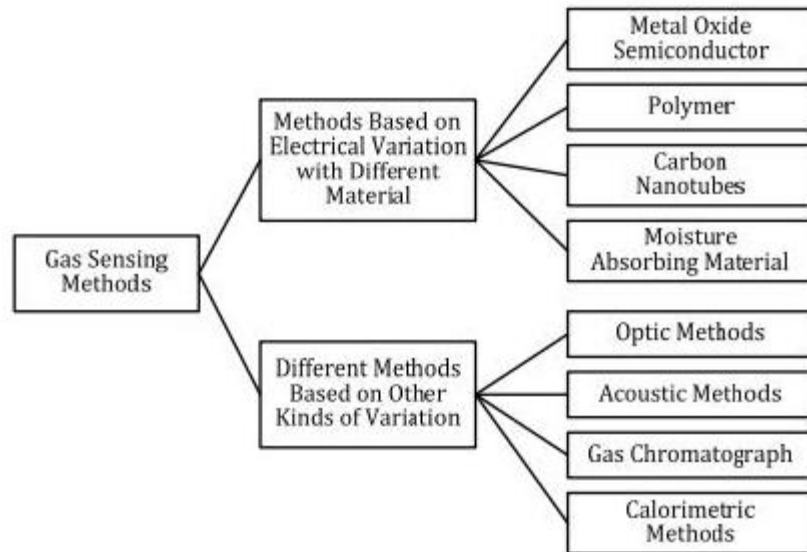


**Figure 1 – Classification of gas sensing methods (Liu 2012)**

Metal oxide semiconductors (MOS) are the most common sensing materials due to advantages such as low cost of production, high sensitivity, and durability (Liu 2012). Fine et al. (2010) discussed the nature of the gas response found in MOS. Absorption or desorption on the surface of a MOS will change the conductivity of the material. To be more useful, the change in conductivity should show some specificity for a specific compound or class of compounds. Since the MOS sensor may respond to several volatile organic compounds in a given molecular class, selectivity can sometimes be an issue and trace levels of contaminants may adversely affect results (Liu 2012).



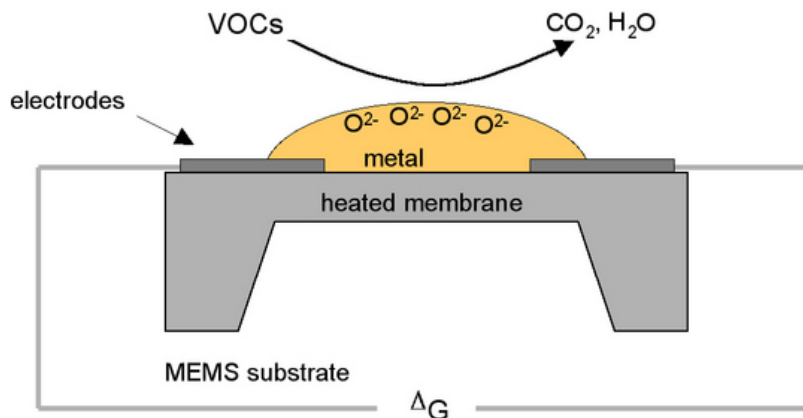


**Figure 2 – MOS sensor principle of operation. Absorption of VOC on surface of heated membrane results in a conductivity change of the sensing material. (BioRegion STERN 2009)**

Optical Sensing Methods are based primarily on spectroscopy and are ideal for real time detection due to a short response time. These sensors work primarily on absorption and emission spectrometry, which is based on Beer-Lambert law. The absorption of photons at specific wavelengths is concentration dependent. This is only the basic method, there are several other improved methods including differential light absorption spectroscopy, tunable diode laser absorption spectroscopy, Raman light detection and ranging, differential absorption, and intra-cavity absorption spectrometry (Liu 2012).

Infrared (IR)-source gas sensors are based on basic absorption spectrometry. An IR-source gas sensor is comprised of an IR source, gas chamber, and an IR detector. The source emits radiation at various wavelengths, including those absorbed by the target gas. An optical filter is used to filter radiation that is not the same wavelength as the target gas wavelength. This allows the target gas to be detected and measured (Liu 2012).

## **Section 2.2 What Makes a Sensor Viable**

A primary objective of this research was to determine the most viable sensor to accomplish the desired goal. In order to compare tested sensors, it was necessary to construct benchmarks for performance evaluation.

Liu et al. (2012) establishes several performance indicators that can be used to determine the viability of a sensor. These indicators are broken down into a list of seven distinct factors: “(1) sensitivity: the minimum detectable value of target gases’ volume concentration when they could be detected; (2) selectivity: the ability of gas sensors to identify a specific gas among a gas mixture; (3) response time: the period from the time when gas concentration reaches a specific value to that when sensor generates a warning signal; (4) energy consumption; (5) reversibility: whether the sensing materials could return to its original state after detection; (6) adsorptive capacity (also affects sensitivity and selectivity); and (7) fabrication cost.” Most of these indicators will be of key importance when evaluating the viability of sensors tested for DEET detection.

“Selectivity” is not a concern for this application. While it is necessary for sensors used in several other applications to be able to detect a specific gas amongst others, the goal of this instrumentation will deal specifically with one VOC.

## **Section 2.3 Detection with Metal Oxide Semiconductor Sensors**

MOS Sensors offer advantages such as low cost and low selectivity. Low cost allows for deployment of several sensors in an array to detect gases at various distances from the sample. Low selectivity allows for detection of a wide range of gases, which is advantageous due the unlikelihood of finding a sensor intentionally designed for

detection of DEET. Low selectivity creates a need to ensure the sensor is not exposed to other VOCs outside the target gas.

However, limitations arise when using MOS sensors for quantitative purposes due to nonlinearity of sensor response, variations in initial resistance, long-term drift, memory effects, and sensitivity to environmental factors such as temperature and relative humidity (Szcurek 2014). These limitations must be taken into consideration when developing a standard operating procedure for sensor evaluations.

Szcurek et al. (2014) subjects a MOS sensor to tests under fluctuating gas concentrations to demonstrate memory effects inherent in using MOS. **Figure 3** shows a MOS sensor response compared to a flame ionization detector (FID) response. Since MOS sensors depend on previous concentration readings as well as present, sensor readings will be erroneous when used for *continuous* monitoring of a fluctuating gas concentration. These sensors are better suited for sampling at certain instances such that the sensor is removed from the gas concentration to allow for stabilization before being exposed to a new level of gas concentration.

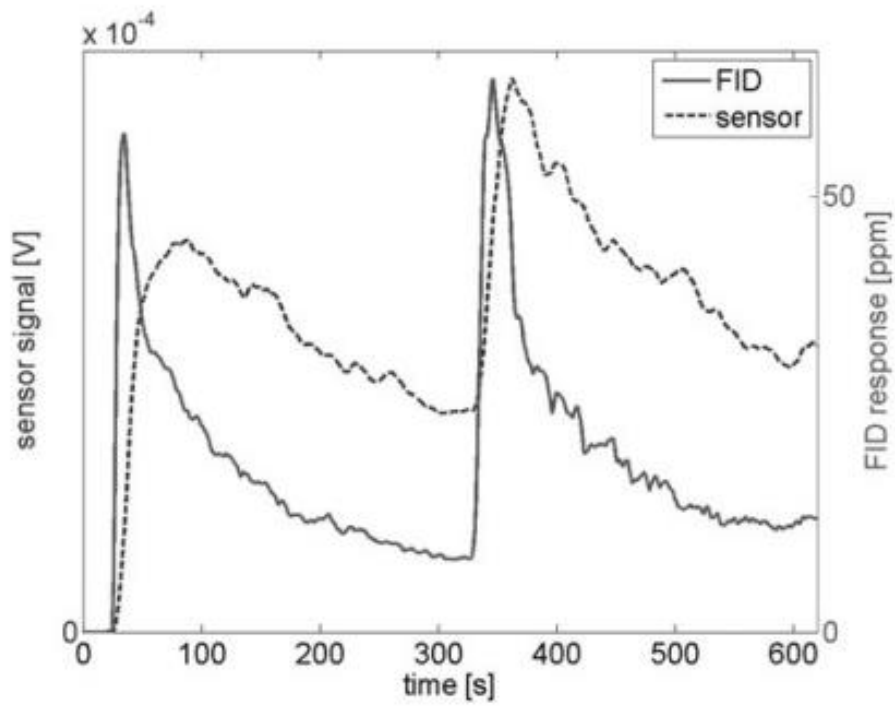


**Figure 3 – MOS response vs FID response. Memory effects of a MOS sensor are evident when compared to an FID response to the same fluctuating gas concentration (Szcurek 2014)**

## Chapter 3 – Methodology

### Section 3.1 Instrumentation Flow

**Figure 4** shows a flow diagram for the general layout of the system with a generic sensor array.

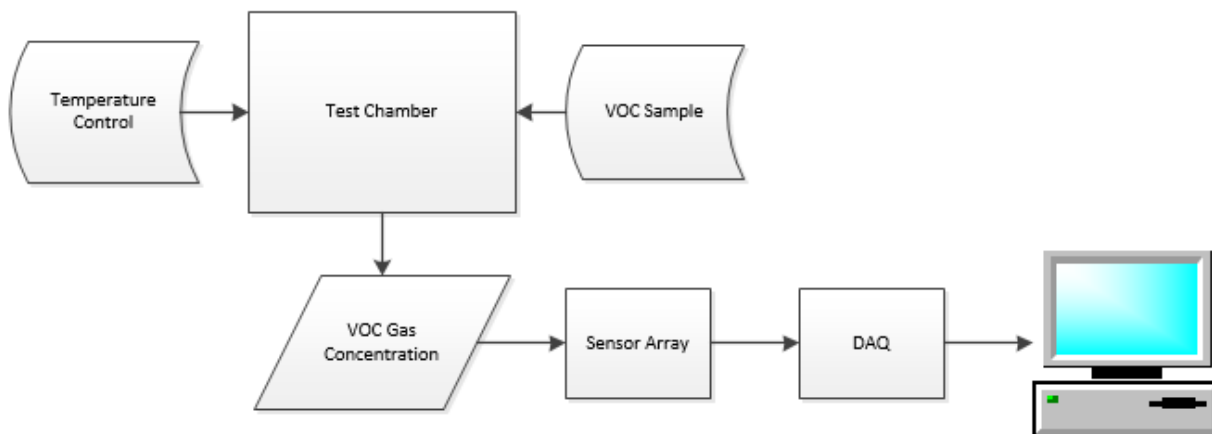


**Figure 4 –General system layout containing all principle parts used in implementation of instrumentation system.**

The test chamber is the controlled test environment where the concentration levels of DEET were measured at varying distances from the surface. The sensor array was housed within this chamber. Sensor readings were monitored using a data acquisition (DAQ) device that transferred data to a computer. Data was processed and recorded using custom software created within LabVIEW.

The temperature level of the test chamber was controlled. Not only can temperature affect the vapor phase concentration and evaporation rate of the DEET, temperature can also affect the values being read by the sensors.

### Section 3.2 Test Chamber Apparatus

To satisfy the need of creating a static testing environment, a custom 200-mL, jacketed flask (shown in **Figure 5**) was used as the test chamber. The jacket allows for temperature-controlled water to circulate through the flask, which kept the temperature of the flask at a constant and repeatable level. Water temperature was allowed to reach the circulated water bath set point before each test.

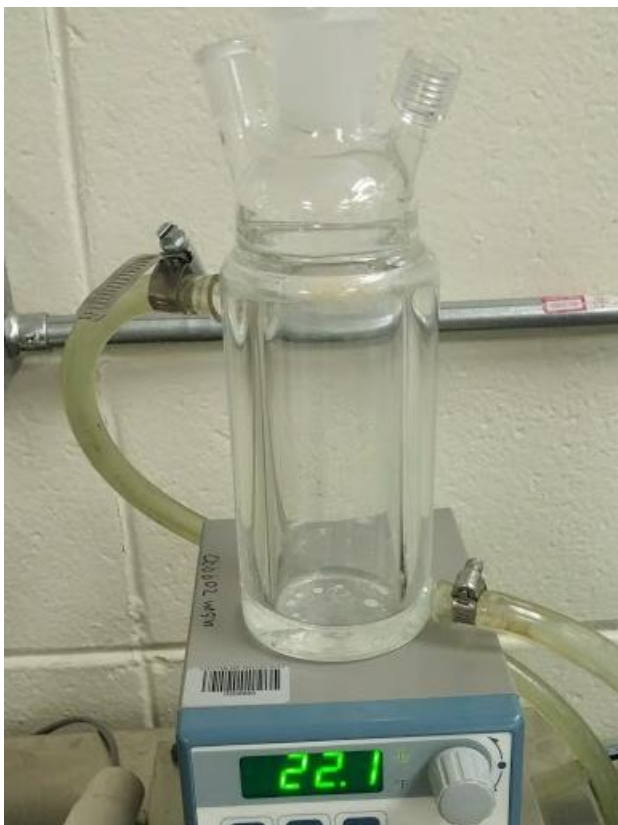


**Figure 5 – Temperature controlled 200 mL jacketed flask used as test chamber.**

The chamber was kept airtight using septa that allowed for insertion of sensors and sample needle into the chamber at adjustable heights.

### Section 3.3 Sensor Testing Methods

For the scope of this project, several MOS sensors were selected for efficacy testing in regards to concentration detection of DEET. Sensors were first selected based

on target gas and signal range. Signal range is necessary to consider because the sensors need to be capable of detecting amounts as low, or lower, than the amounts being monitored for this experiment. The low vapor pressure of DEET, only  $5.6 \times 10^{-3}$  mmHg at 20 °C (Jackson 2008), causes the compound to evaporate at a slower rate, resulting in detection challenges when compared with more volatile organic compounds. Thus, the sensor must be sensitive enough to monitor low ppm concentrations.

Initially, sensors were screened based on response to DEET over a short period of time (~3 minutes). For the scope of this thesis, two types of MOS sensors were selected for a case study based on successful screening response. An array of three sensors of the selected type underwent testing at three distances from the sample, with each sensor placed at the same distance from the sample during each test. The temperature within the jacket was set to 25 °C, and 50  $\mu$ L of DEET was introduced into the bottom of the chamber using a needle. The sensor was exposed to the sample for 15 minutes in each test.

In order to evaluate the performance of the sensors, a set of quantifiable benchmarks were used to compare the efficacy of different sensors and sensor configurations. Sensors were compared based on repeatability and degradability. Case study sensors needed to undergo the same test conditions including environmental conditions and number of tests. The repeatability of the sensor was quantified by calculating the deviation of the measurements under repeat test conditions (i.e. same height).

### Section 3.4 Sensor Circuitry

A MOS sensor must be heated using a resistive heating element in order for the sensor membrane material to reach desirable operating characteristics. The power dissipated by this element is provided in the datasheet of each sensor, and a suitable supply voltage was used to obtain this dissipation. According to manufacturer specifications, sensors often must undergo an initial preheat conditioning phase of several days, as well as a short preheat phase before each test. Each sensor was heated according to specification to ensure a steady baseline was reached before exposure to gas concentration.

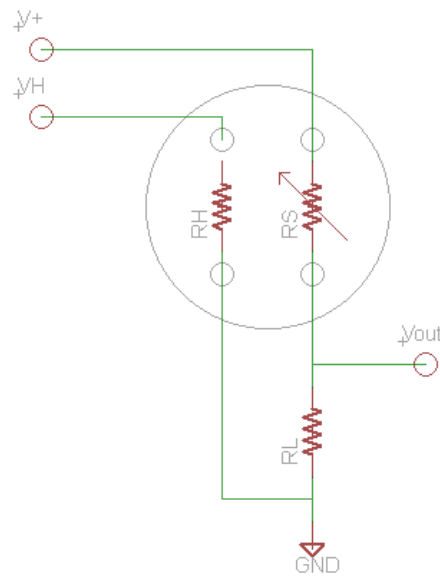


**Figure 6 – Basic MOS sensor circuit to monitor the ratio between load resistance and sensor resistance.**

As discussed in the Literature Review, the resistance of the sensor membrane is inversely proportional to the gas concentration present. Thus, a basic voltage divider circuit (**Figure 6**) was used to monitor the resistance of the sensor. The output voltage response ( $V_{out}$ ) is given by the equation



$$V_{out} = \frac{R_L}{R_S + R_L} V_+$$

**Equation 1 – Voltage Divider 1**

where  $R_L$  is the load resistance,  $R_S$  is the sensor resistance, and  $V_+$  is the sensing voltage.

This equation can be rearranged to calculate the sensor membrane resistance ( $R_S$ ) as shown in **Equation 2**.

$$R_S = \frac{V_+ - V_{out}}{V_{out}} R_L$$

**Equation 2 – Voltage Divider 2**

Output voltage is inversely proportional to sensor resistance. **Figure 7** shows this relationship plotted in MATLAB for parameters of a typical MOS sensor with a 10 kΩ load resistor.

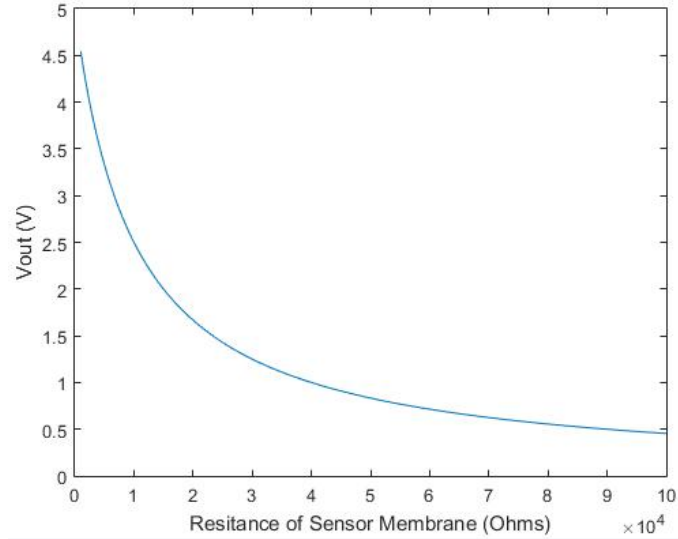


**Figure 7 – Curve for output voltage as a function of sensor resistance as defined by the voltage divider equation (Equation 2).**

Note that due to resolution limitations imposed during digital to analog conversion (DAC) performed by the DAQ device, it is desirable to operate within a range that will produce a significant voltage change per change in sensor resistance. If a test were

performed in the lower voltage range (i.e.  $V_{out} < 0.6 V$ ), a larger sensor resistance change would need to occur before becoming evident by the voltage output response. Likewise, if a test were performed in the upper range, there is higher risk that the sensor voltage output will be saturated (i.e.  $V_{out} = V_+$ ). Thus, the load resistor was adjusted such that  $V_{out}$  was between  $0.8 V$  and  $1.3 V$  at the start of each test run.

### Section 3.5 Data Acquisition and Processing

To monitor the voltage output, analog inputs on the NI PXI-6251 multifunction DAQ device were used. This DAQ device was chosen based on availability and high input impedance ( $> 10 G\Omega$ ), which is necessary to interface with the wide impedance range of some MOS sensors without introducing loading effects. **Figure 8** shows the custom program developed in LabVIEW used to process the data.

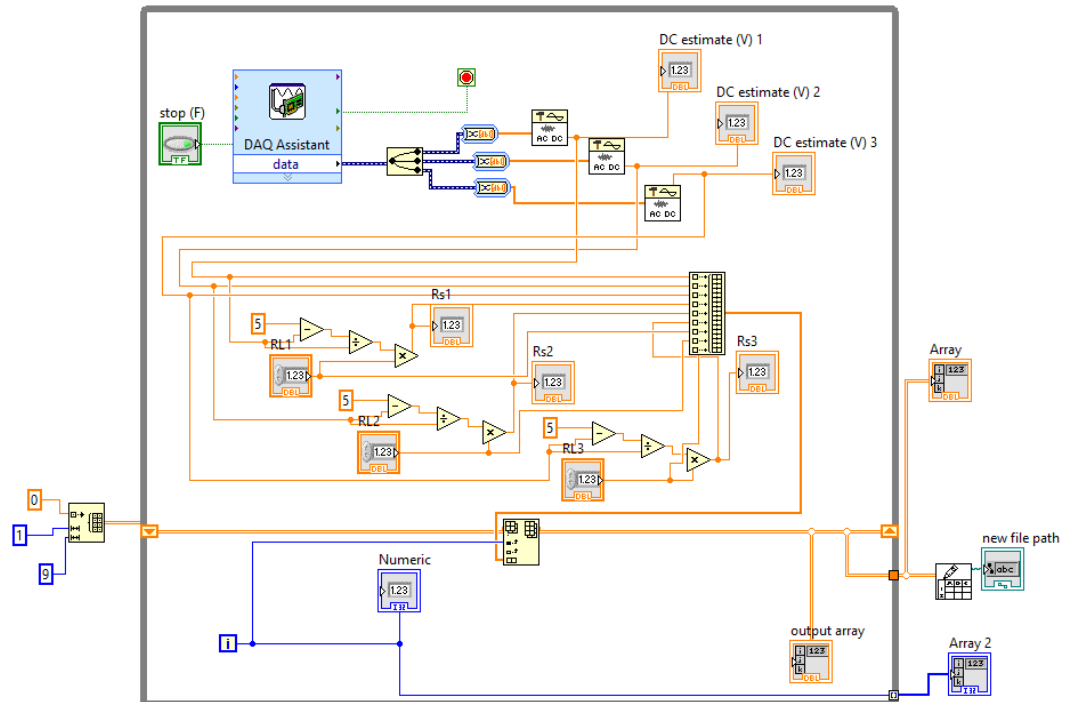


**Figure 8 - LabVIEW block diagram for software used in data processing and exportation to CSV.**

This program samples a differential voltage measurement ( $V_{out}$ ) 100 times at a rate of 100 Hz. (100,000 samples per second). A Hamming Window variant is used to average these data points and output 1 data point each second. The duration of each test lasts 15 minutes after introduction of the sample, meaning each test will output 930 voltage data points per sensing circuit. These data points are stored in an array, which is exported to a comma separated value (CSV) file.

The program also allows the user to input the load resistance value for each sensing circuit. This value is then used in conjunction with **Equation 2** to calculate the sensor resistance at each voltage data point and export to the same CSV. Each output file contains the voltage response, sensor resistance, and load resistance for each sensing circuit.

Voltage response is a function of sensor resistance and load resistance, as shown in **Figure 7**. LabVIEW converts the output voltage response to the sensor resistance response; this transformation is shown in **Figure 9** and **Figure 10**.

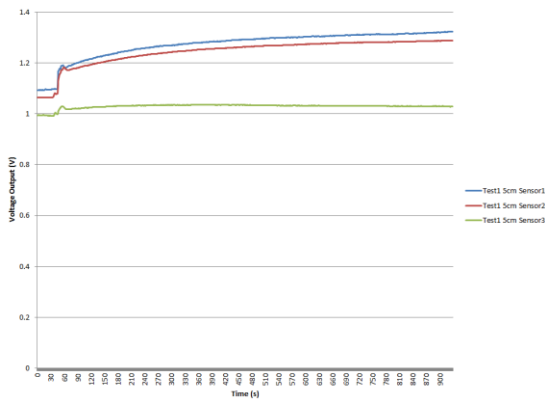


**Figure 9 – Typical sensor voltage response recorded under standard screening protocol for a period of 15 minutes.**

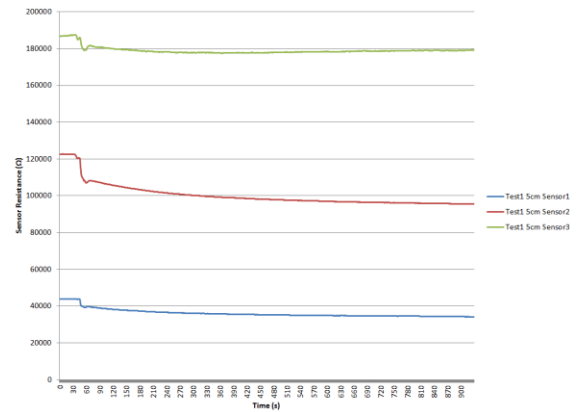


**Figure 10 – Typical sensor resistance response recorded under standard screening protocol for a period of 15 minutes.**

Initial resistances can vary widely even among sensors of the same model. To compare sensor responses, the responses were normalized using **Equation 3**

$$N(t) = \frac{R_0}{R_s(t)}$$

### **Equation 3 – Sensor Resistance Normalization**

where  $R_0$  is defined as the initial resistance before sample exposure at  $t = 25$  s and  $R_s(t)$  is the recorded sensor resistance response as a function of time.

In order to characterize sensor response, a first order exponential decay function (**Equation 4**) was used to approximate the response. Time constant  $k$  will be averaged over a specified response range.  $N_{min}$  is the lowest resistance reading in the chosen response range.

$$N - N_{min} = N_0 e^{kt}$$

### **Equation 4 – First Order Exponential Decay**

## Chapter 4 – Data Analysis

After the initial screening process, two MOS sensors models were selected for case studies: the TGS 2602 by Figaro and the UltraKera P/N 731 by Synkera. Each model of sensor was configured as an array of three at the same height. The response of each array was recorded at 5 cm distance, 3 cm distance, and 1 cm distance. This was repeated three times, meaning 9 tests and 27 sensor responses for each model.

### Section 4.1 – Sensor Resistance Response

Sensor resistance was plotted as a function of time over the entire test duration.

**Figure 11, 12, 13, 14, 15, and 16** show sensor resistance responses for each sensor model at each distance.

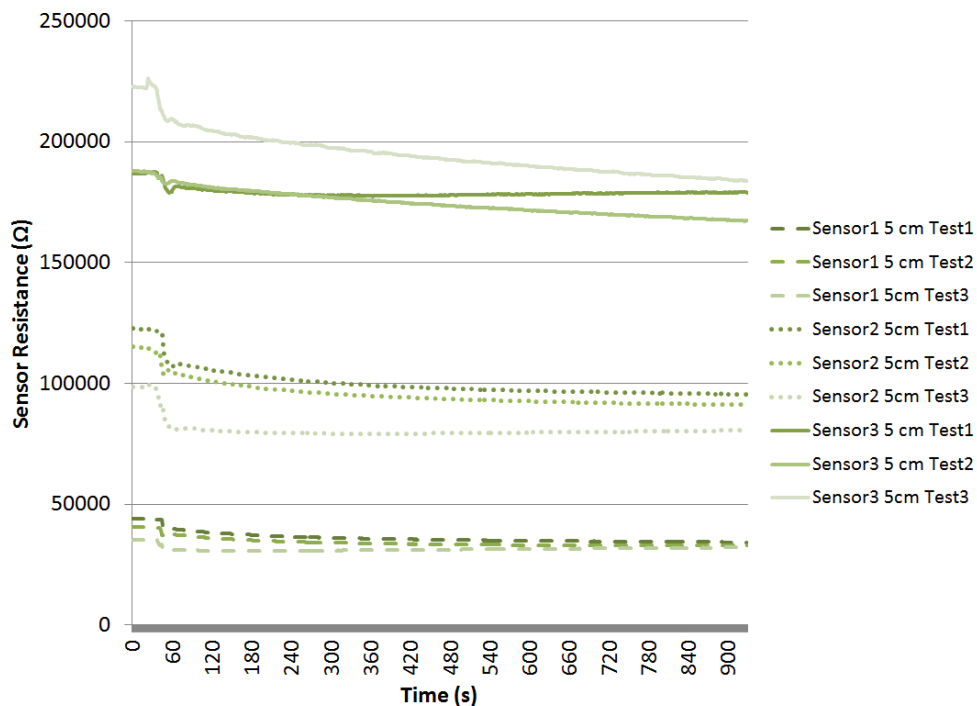


**Figure 11 – UltraKera 731 sensor resistance responses to 50 µL of DEET at 25 °C; 5 cm above sample.**

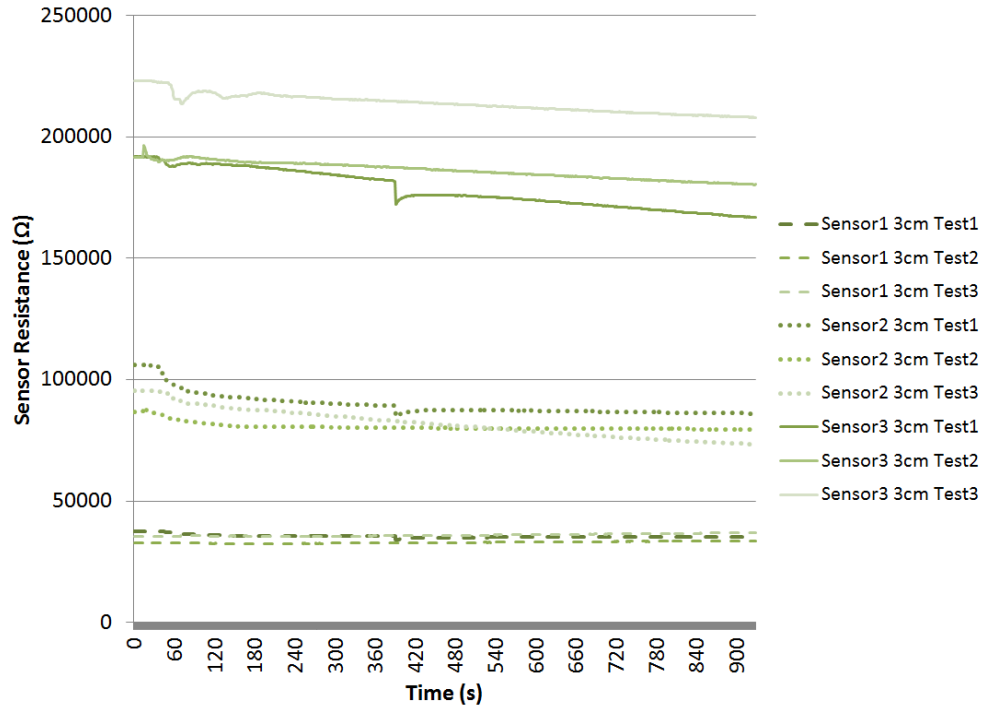


**Figure 12 – UltraKera 731 sensor resistance responses to 50  $\mu\text{L}$  of DEET at 25  $^{\circ}\text{C}$ ; 3 cm above sample.**

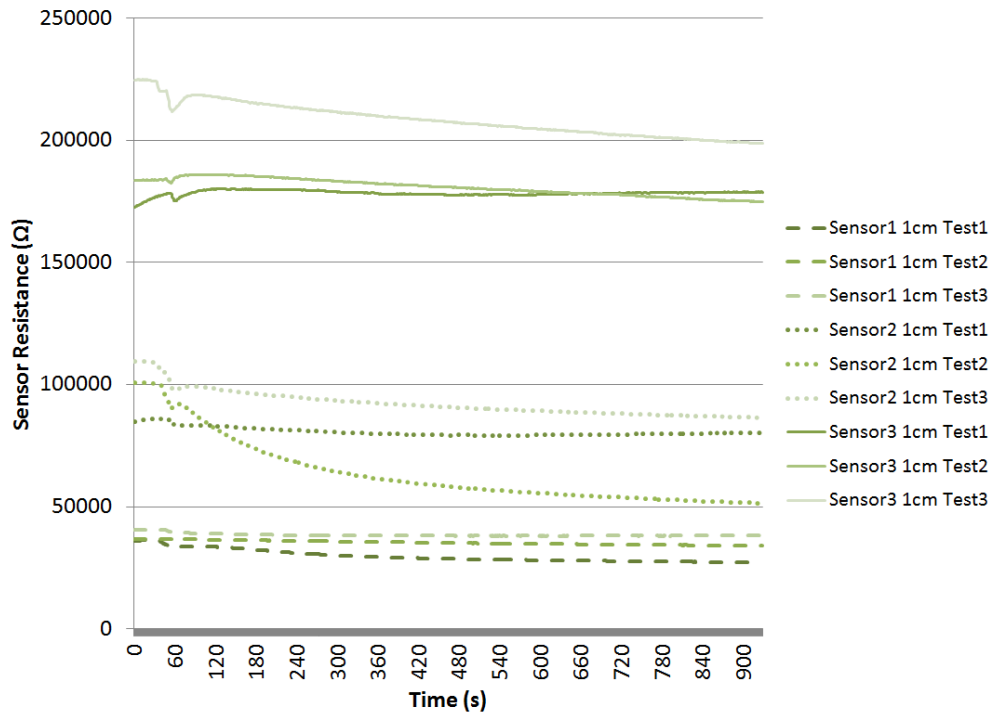


**Figure 13 – UltraKera 731 sensor resistance responses to 50  $\mu\text{L}$  of DEET at 25  $^{\circ}\text{C}$ ; 1 cm above sample.**

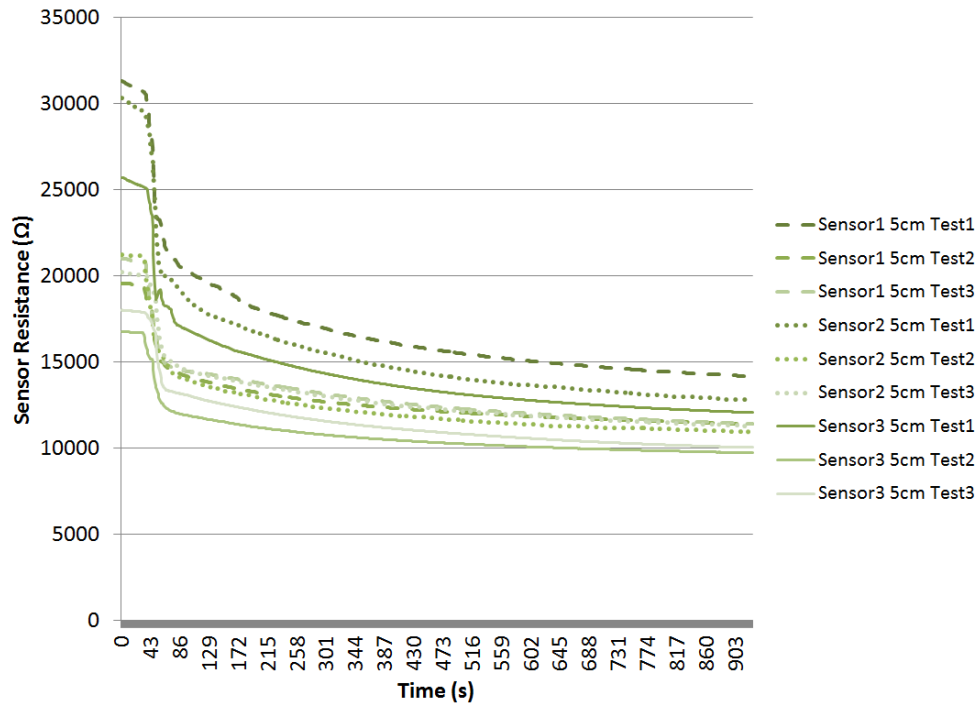


**Figure 12 – TGS 2602 sensor resistance responses to 50 µL of DEET at 25 °C; 5 cm above sample.**

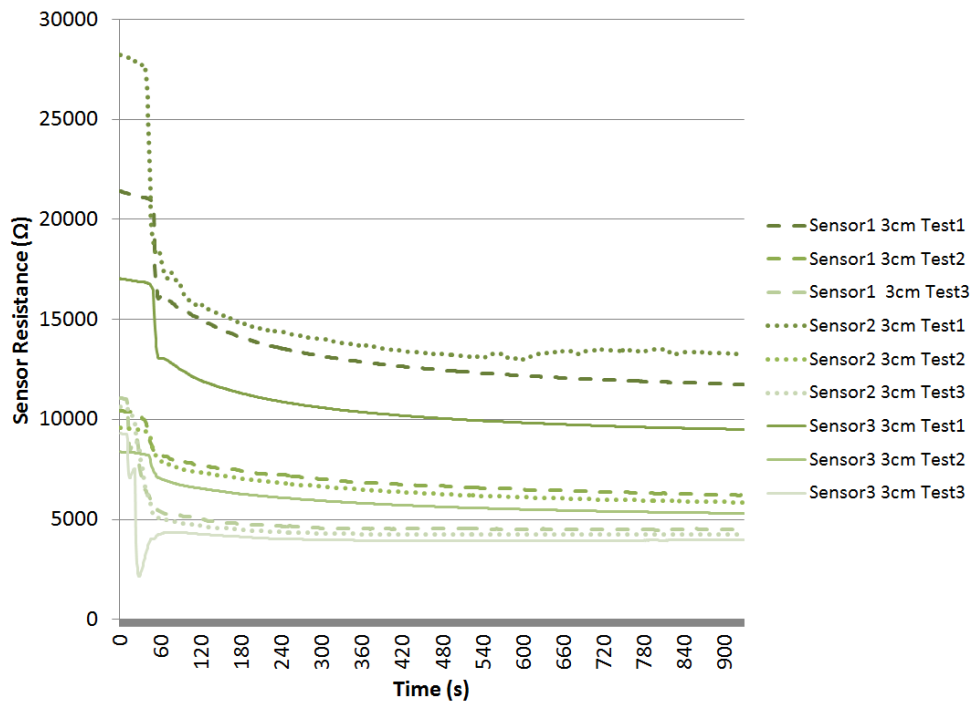


**Figure 13 – TGS 2602 sensor resistance responses to 50 µL of DEET at 25 °C; 3 cm above sample.**

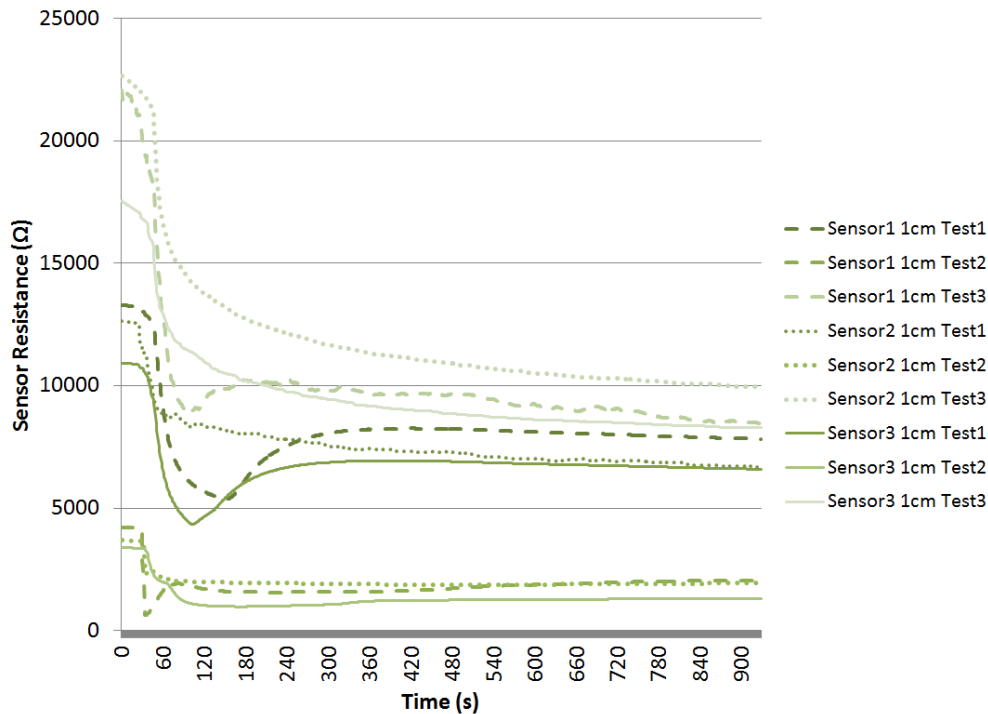


**Figure 14 – TGS 2602 sensor resistance responses to 50 µL of DEET at 25 °C; 1 cm above sample.**

#### Section 4.2 Normalization

Sensor resistance response was normalized using **Equation 3** in order to compare sensors of the model. The average response was calculated at  $t = 90s$  to compare sensor step response after exposure to the sample. Percent deviation from this average was calculated for each test run.



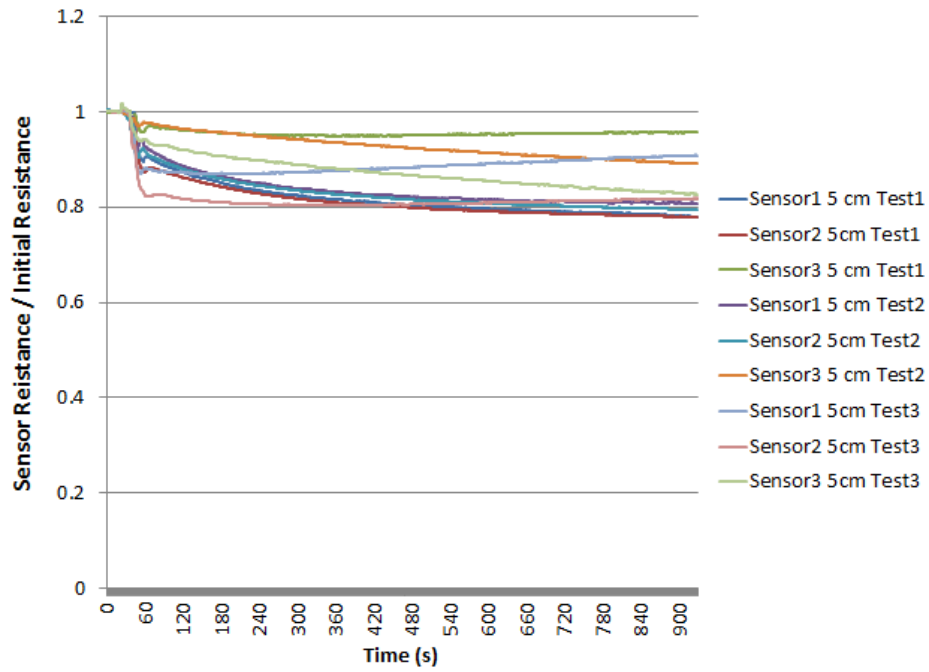


**Figure 17 – UltraKera 731 normalized responses to 50 µL of DEET at 25 °C; 5 cm above sample.**

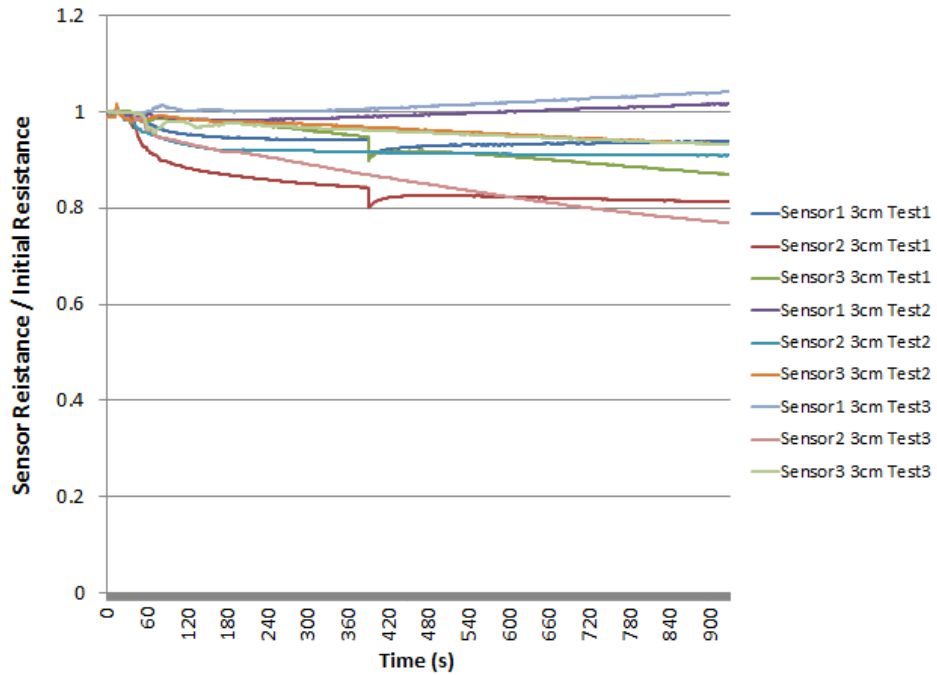


**Figure 18 - UltraKera 731 normalized responses to 50 µL of DEET at 25 °C; 3 cm above sample.**

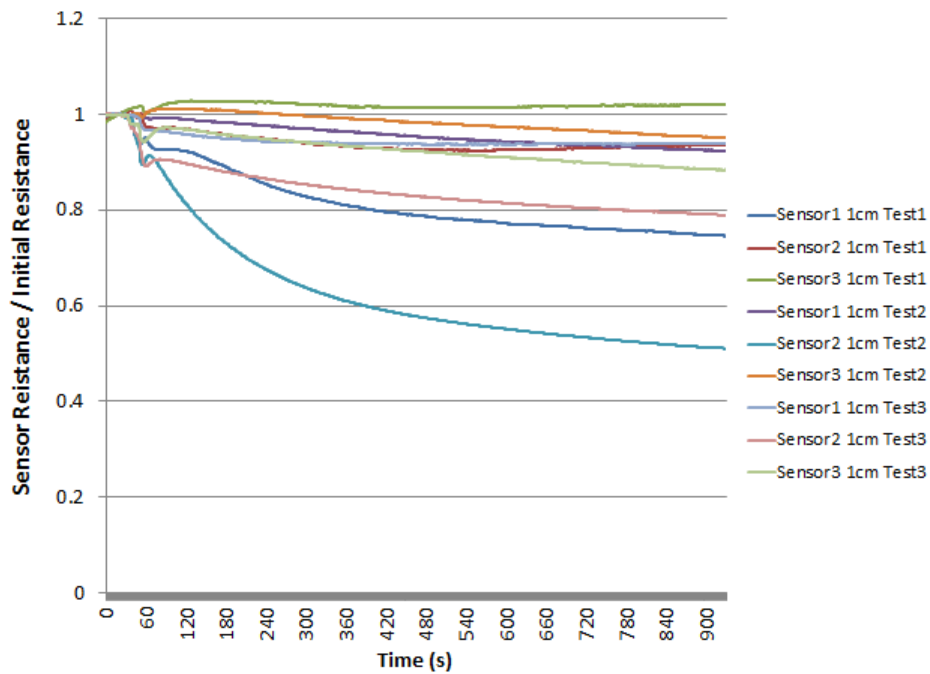


**Figure 19 - UltraKera 731 normalized responses to 50  $\mu$ L of DEET at 25  $^{\circ}$ C; 1 cm above sample.**

**Data Table 1 – UltraKera 731 Average Response at t = 90s**

	5 cm	3 cm	1 cm
Average $N(90)$	0.9036	0.9667	0.9596
Standard Deviation	0.0460	0.0343	0.0494

**Data Table 2 – UltraKera Percent Deviation at t = 90s**

	5 cm	3 cm	1 cm
Sensor 1 Test 1	-1.57 %	-0.61 %	-3.47 %
Percent Deviation			
Sensor 1 Test 2	0.08 %	2.35 %	3.52 %
Percent Deviation			
Sensor 1 Test 3	-3.14 %	4.45 %	0.44 %
Percent Deviation			
Sensor 2 Test 1	-3.14 %	-7.15 %	1.29 %
Percent Deviation			
Sensor 2 Test 2	-0.85 %	-2.51 %	-9.11 %
Percent Deviation			
Sensor 2 Test 3	-8.60 %	-2.32 %	-5.65 %
Percent Deviation			
Sensor 3 Test 1	6.90 %	1.99 %	6.32 %
Percent Deviation			
Sensor 3 Test 2	7.39 %	2.54 %	5.34 %
Percent Deviation			
Sensor 3 Test 3	2.92 %	1.21 %	1.36 %
Percent Deviation			

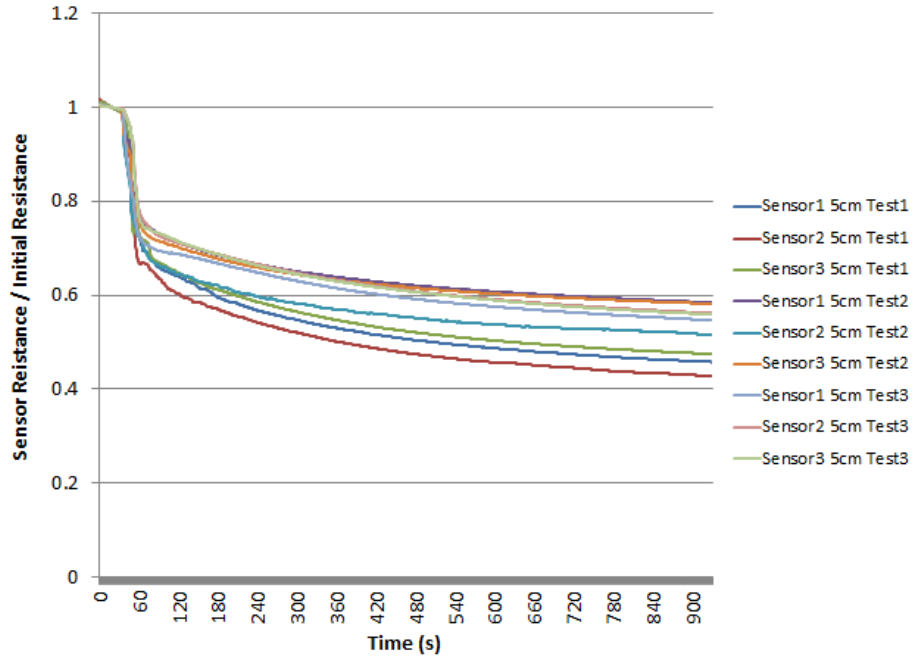


**Figure 20 – TGS 2602 normalized responses to 50 µL of DEET at 25 °C; 5 cm above sample.**

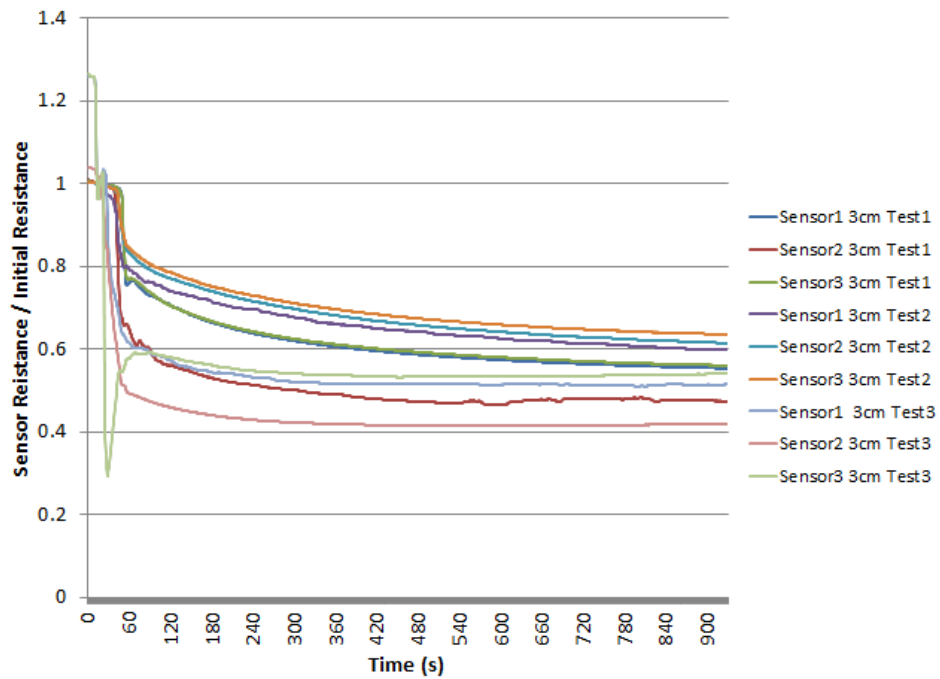


**Figure 21 – TGS 2602 normalized responses to 50 µL of DEET at 25 °C; 3 cm above sample.**

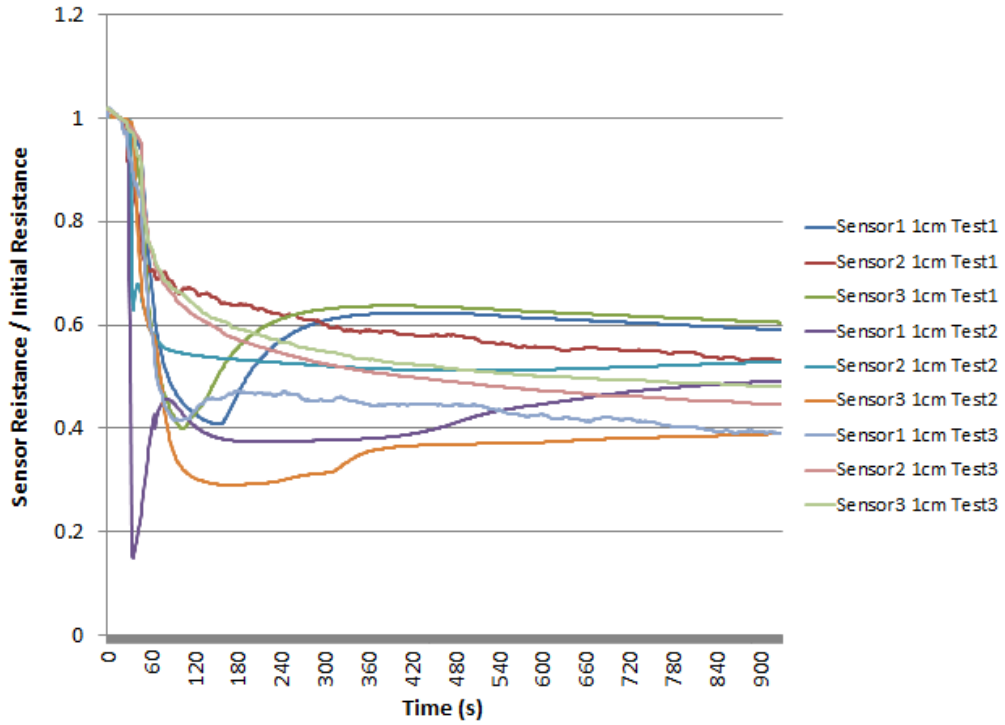


**Figure 22 – TGS 2602 normalized responses to 50 µL of DEET at 25 °C; 1 cm above sample.**

**Data Table 3 – TGS 2602 Average Response at t = 90s**

	5 cm	3 cm	1 cm
Average $N(90)$	0.6927	0.6771	0.5236
Standard Deviation	0.0358	0.1148	0.1220

**Data Table 4 – TGS 2602 Percent Deviation at t = 90s**

	5 cm	3 cm	1 cm
Sensor 1 Test 1	-4.74 %	7.94 %	-7.92 %
Percent Deviation			
Sensor 1 Test 2	5.56 %	12.70 %	-13.70 %
Percent Deviation			
Sensor 1 Test 3	0.34 %	-12.29 %	-19.57 %
Percent Deviation			
Sensor 2 Test 1	-7.99 %	-11.11 %	30.59 %
Percent Deviation			
Sensor 2 Test 2	-4.01 %	17.15 %	5.05 %
Percent Deviation			
Sensor 2 Test 3	5.01 %	-29.92 %	26.10 %
Percent Deviation			
Sensor 3 Test 1	-3.27 %	9.12 %	-17.99 %
Percent Deviation			
Sensor 3 Test 2	3.34 %	19.17 %	-30.76 %
Percent Deviation			
Sensor 3 Test 3	5.76 %	-12.76 %	28.19 %
Percent Deviation			

### Section 4.3 Exponential Approximation

Sensor response curves were approximated using a first order exponential decay function between 30 and 90 seconds.

**Data Table 5 – UltraKera 731 Time Constants**

	5 cm	3 cm	1 cm
Sensor 1 Test 1 <i>k</i>	-0.22277	-0.28017	-0.25962
Sensor 1 Test 2 <i>k</i>	-0.23227	-0.43189	-0.40387
Sensor 1 Test 3 <i>k</i>	-0.23577	-0.52325	-0.30372
Sensor 2 Test 1 <i>k</i>	-0.22392	-0.22698	-0.31370
Sensor 2 Test 2 <i>k</i>	-0.23785	-0.28023	-0.19807
Sensor 2 Test 3 <i>k</i>	-0.21535	-0.26024	-0.22996
Sensor 3 Test 1 <i>k</i>	-0.28839	-0.35137	-0.28425
Sensor 3 Test 2 <i>k</i>	-0.33751	-0.43938	-0.39263
Sensor 3 Test 3 <i>k</i>	-0.26334	-0.27216	-0.26901

**Data Table 6 – UltraKera 731 Time Constant Average**

	5 cm	3 cm	1 cm
Average <i>k</i>	-0.25080	-0.34063	-0.29498
Standard Deviation	0.03967	0.10181	0.06844

**Data Table 7 UltraKera 731 Time Constant Percent Deviation**

	5 cm	3 cm	1 cm
Sensor 1 Test 1 Percent	-11.18%	-17.75%	-11.99%
Deviation			
Sensor 1 Test 2 Percent	-7.39%	26.79%	36.91%
Deviation			
Sensor 1 Test 3 Percent	-5.99%	53.61%	2.96%
Deviation			
Sensor 2 Test 1 Percent	-10.72%	-33.36%	6.35%
Deviation			
Sensor 2 Test 2 Percent	-5.16%	-17.73%	-32.85%
Deviation			
Sensor 2 Test 3 Percent	-14.13%	-23.60%	-22.04%
Deviation			
Sensor 3 Test 1 Percent	14.99%	3.15%	-3.64%
Deviation			
Sensor 3 Test 2 Percent	34.57%	28.99%	33.10%
Deviation			
Sensor 3 Test 3 Percent	5.00%	-20.10%	-8.80%
Deviation			



**Data Table 8 – TGS 2602 Time Constants**

	5 cm	3 cm	1 cm
Sensor 1 Test 1 <i>k</i>	-0.13169	-0.14706	-0.08392
Sensor 1 Test 2 <i>k</i>	-0.15572	-0.17478	-0.18098
Sensor 1 Test 3 <i>k</i>	-0.15274	-0.17059	-0.08602
Sensor 2 Test 1 <i>k</i>	-0.13057	-0.13514	-0.17144
Sensor 2 Test 2 <i>k</i>	-0.14335	-0.16640	-0.15972
Sensor 2 Test 3 <i>k</i>	-0.14321	-0.15315	-0.12460
Sensor 3 Test 1 <i>k</i>	-0.13504	-0.14703	-0.08171
Sensor 3 Test 2 <i>k</i>	-0.15567	-0.17143	-0.07228
Sensor 3 Test 3 <i>k</i>	-0.15439	-0.11684	-0.13074

**Data Table 9 – TGS 2602 Time Constant Average**

	5 cm	3 cm	1 cm
Average <i>k</i>	-0.14471	-0.15360	-0.12127
Standard Deviation	0.01041	0.01936	0.04223

**Data Table 10 – TGS 2602 Time Constant Percent Deviation**

	5 cm	3 cm	1 cm
Sensor 1 Test 1 Percent	-9.00%	-4.26%	-30.80%
Deviation			
Sensor 1 Test 2 Percent	7.61%	13.79%	49.24%
Deviation			
Sensor 1 Test 3 Percent	5.55%	11.06%	-29.07%
Deviation			
Sensor 2 Test 1 Percent	-9.77%	-12.02%	41.38%
Deviation			
Sensor 2 Test 2 Percent	-0.94%	8.33%	31.70%
Deviation			
Sensor 2 Test 3 Percent	-1.03%	-0.30%	2.75%
Deviation			
Sensor 3 Test 1 Percent	-6.68%	-4.28%	-32.62%
Deviation			
Sensor 3 Test 2 Percent	7.58%	11.60%	-40.40%
Deviation			
Sensor 3 Test 3 Percent	6.69%	-23.93%	7.81%
Deviation			

## Chapter 5 – Discussion of Results and Conclusions

Sensors of the same model were expected to be from the same batch and thus share similar initial membrane resistance values. However, as shown for UltraKera 731, starting resistances varied from 40 k $\Omega$  to 180 k $\Omega$ . Normalization of sensor response provided a common scale to compare sensors of varying resistances without construing the curve of the sensor response.

To create a metric for sensor repeatability, the normalized response at  $t = 90s$  was averaged at each height, and the percent deviation from this average was calculated for each sensor response. UltraKera 731 normalized responses showed high repeatability, with all response values being within  $\pm 10\%$  of the average for all sensor heights. TGS 2602 showed much less repeatability, with sensor responses varying up to  $\pm 30\%$ . As shown by **Data Table 1** and **Data Table 3**, deviation from the mean was consistently greatest at 1 cm distance from the sample. This suggests either: 1) an inconsistent vapor phase concentration present that close to the sample or 2) degradation of the sensing material during the 1 cm tests.

Absorption of vapor-phase VOCs on the sensor membrane decreases the resistance of the sensor. Thus, a higher concentration of the target gas results in a higher resistance change in the sensor membrane. Assuming concentration of gas molecules is inversely proportional to distance from the sample, normalized response of UltraKera 731 at  $t = 90s$  did not distinguish between concentrations present under test conditions of this scope despite high repeatability. Average normalized sensor response was greatest at 5 cm, the furthest distance from the sensor. Unlike the UltraKera 731, the TGS 2602

followed the expected response, with the average normalized sensor response being greatest at 1 cm and least at 5 cm. However, as shown by **Data Table 3**, the deviation is large enough that responses at various distances overlap and thus may not be repeatable.

Curve approximation using a first order exponential decay function was proposed as a method to provide a more precise metric to characterize sensor response than looking at the total change in sensor resistance between two data points. This was accomplished by averaging the time constant for all data points within the specified range of the curve (between  $t = 30s$  and  $t = 90s$ ).  $t = 30s$  was chosen as the starting time because sensor response begins shortly after introduction of the sample.  $t = 90s$  was selected because the rate of change of most sensor response curves approached zero at that time. The entire response was not approximated because in most cases the time constant would decrease in magnitude significantly and valuable information about the initial curve response would be lost if all data points were included in this average. This average time constant approximation method was chosen over selection of critical points (local maxima, local minima, points of inflection, etc.) because of variances in sensor response that did not produce consistent key features across all data sets.

Referring back to MOS sensor principle of operation, it can be expected that a higher rate of sensor resistance change will correlate to a higher gas concentration. At 5 cm, the UltraKera 731 and TGS 2602 average time constants were  $-0.25080 \pm 0.03967$  and  $-0.14471 \pm 0.01041$  respectively. Comparing these values to the time constant at 3 cm for UltraKera 731 ( $-0.34063 \pm 0.10181$ ) and TGS 2602 ( $-0.15360 \pm 0.01936$ ) suggests the concentration gradient present between 5 cm and 3 cm is detectable by these sensors. Both sensors show an increased average rate of change magnitude when transitioning

from 5 to 3 cm. However, this trend did not hold true for 1 cm tests. As evident by variance in the normalized response, neither sensor responded well under 1 cm conditions

Although resistance of the sensor membrane is directly proportional to gas concentration, analysis of sensor resistance at select data points did not reliably distinguish a concentration gradient between distances across multiple test runs. Thus, it was necessary to take into account average rate of change of the sensor response using the proposed curve approximation method. This method successfully distinguished between 5 cm and 3 cm distances, but failed to do so at the 1 cm distance. Sensor placement at 1 cm is likely too close to the sample to accurately measure gas concentration due to inconsistent vapor phase sampling. Future sensor testing should be done at greater distances to confirm the relationship of time constant to gas concentration.

## Works Cited

- Achee, Nicole L.; Bangs, Michael J.; Farlow, Robert; Killeen, Gerry F; Lindsay, Steve; Logan, James G; Moore, Sarah J.; Rowland, Mark; Sweeney, Kevin; Torr, Steve J.; Zwiebel, Laurence J. and Grieco, John P. "Spatial Repellents: from Discovery and development to evidence-based validation." *Malaria Journal*, 14 May 2012.
- "AppliedSensor GmbH – Chemical Gas Sensors to Detect Contaminants."  
[www.gesundheitsindustrie-bw.de](http://www.gesundheitsindustrie-bw.de). BioRegio STERN, 9 December 2009. Web.
- Fine, George F.; Cavanagh, Leon M.; Afonja, Ayo and Binions, Russell. *Metal Oxide Semi-Conductor Gas Sensors in Environmental Monitoring*. Department of Chemistry, University College London. 1 June 2010.
- Jackson D.; Luukinen, B.; Buhl, K. and Stone, D. "DEET Technical Fact Sheet."  
[npic.orst.edu/factsheets/archive/DEETtech.html](http://npic.orst.edu/factsheets/archive/DEETtech.html). National Pesticide Information Center, Oregon State University Extension Services, July 2008. Web.
- Katz, Tracy M.; Miller, Jason H. and Hebert, Adelaide A. "Insect Repellents: Historical Perspectives and New Developments." *Journal of the American Academy of Dermatology*, 10 May 2007.
- Kish, L.B.; Vajtai, R. and Granqvist, C.G. "Extracting information from noise spectra of chemical sensors: single sensor electronic noses and tongues" *The Angstrom Laboratory*, Uppsala University. 20 June 2000.
- Liu, Xiao; Cheng; Sitian; Liu, Hong; Hu, Sha; Zhang, Daqiang and Ning, Huansheng. A survey on gas sensing technology. *Sensors*, 12(7):9635–9665, 2012.

- Netchaev, Anton. "Selective Detection of Volatile Organic Compounds Using Metal Oxide Sensor Arrays." The University of Southern Mississippi. December 2014.
- Stetter, Joseph R. and Penrose, William R. "Understanding Chemical Sensors and Chemical Sensor Arrays (Electronic Noses): Past, Present, and Future." WILEY-VCH Verlag. 4 February 2002.
- Szczurek, Andrzej; Badura, Marek; Banaszkiewicz, Kamil; Maciejewska, Monika and Marcinkowski, Tadeusz. "Monitoring Volatile Organic Compound Emission Based on Semiconductor Gas Sensors." Environmental Engineering Science, 1 October 2014.